

# Polarization Observations of the OH Maser W75N on the Nançay Radio Telescope

V. I. Slysh<sup>†1</sup>, M. I. Pashchenko<sup>2</sup>, G. M. Rudnitskii<sup>2</sup>, V. M. Vitrishchak<sup>2</sup>, and P. Colom<sup>3</sup>

<sup>1</sup>Astro Space Center, Lebedev Physical Institute, Russian Academy of Sciences,  
Prosoyuznaya ul. 84/32, Moscow, 117997 Russia

<sup>2</sup>Sternberg Astronomical Institute, Moscow State University,  
Universitetskii pr. 13, Moscow, 119991 Russia

<sup>3</sup>LESIA, Observatoire de Paris, Section de Meudon, 5 place Jules Janssen,  
92195 Meudon CEDEX, France

Received October 20, 2009; in final form, November 26, 2009

**Abstract**—Results of observations of the OH maser in W75N at 18 cm are reported. The observations were obtained on the radio telescope of the Nançay Radio Astronomy Observatory (France) from October 2007 to April 2009. The profiles of the Stokes parameters  $I$ ,  $Q$ ,  $U$ , and  $V$  in the 1665 and 1667 MHz OH lines have been measured. A technique taking into account instrumental polarization has been developed and applied. The emission in the OH lines is strongly polarized both linearly and circularly. The degree of polarization of some emission features reaches almost 100%. There were two flares of the maser emission in 2008–2009. During a flare at a radial velocity of +5.5 km/s, a Zeeman pattern was detected in the 1667 MHz line. The measured intensity of the line-of-sight component of the magnetic field was  $-1.1$  mG, which corresponds to the field being directed away from the observer. The maser flares and the associated enhancement of the magnetic field could be associated with the compression of gas at a shock front.

**DOI:** 10.1134/S1063772910070048

## 1. INTRODUCTION

Magnetic fields play an important role at all stages of the star-formation process. Initially, magnetic fields considerably enhance the efficiency of the formation of giant molecular clouds via coalescence. Magnetized clouds can move only along magnetic field lines, making their motion one-dimensional; thus, the probability of collision and coalescence of clouds increases compared to the case of three-dimensional motion in the absence of a magnetic field.

During the fragmentation of giant molecular clouds, magnetic fields, together with rotation, substantially modify the process of the collapse and accretion of material onto the central protostar. Since rotational centrifugal forces increase near the central condensation (protostar), the growth of the mass due to the inflow of material is slowed, hindering the formation of very massive stars. Magnetic fields can efficiently brake the rotation, allowing matter to fall freely onto the protostar. In addition, the magnetic field may prolong the accretion stage, enabling protostars to acquire masses corresponding to those of OB main-sequence stars, i.e., more than  $8 M_{\odot}$ .

Braking the rotation of the inner regions results in the transfer of angular momentum from the core to the disk surrounding the protostar. The circumstellar disk can subsequently provide material for the formation of protoplanets.

Observations can provide information about the intensity and direction of the magnetic fields in star-forming regions, through the polarization of the emission. Lines of the OH molecule, in particular, the main lines of the ground state, are sensitive indicators of the magnetic field. A large number of masers associated with star-forming regions are observed in these lines. In a magnetic field, the lines are split by the Zeeman effect, which induces both circular and linear polarization of the maser emission [1, 2]. The pattern of the Zeeman splitting of the ground-state levels of the OH molecule is considered in detail in [3].

Recently a number of observational studies of the polarization of OH maser emission have been carried out [4–9]. The detection of the Zeeman pattern in the profiles of polarized maser emission enables estimation of the magnetic fields in the sources. The measured fields reach several milliGauss, which is two to three orders of magnitude higher than the mean field in the interstellar medium.

<sup>†</sup>Deceased.

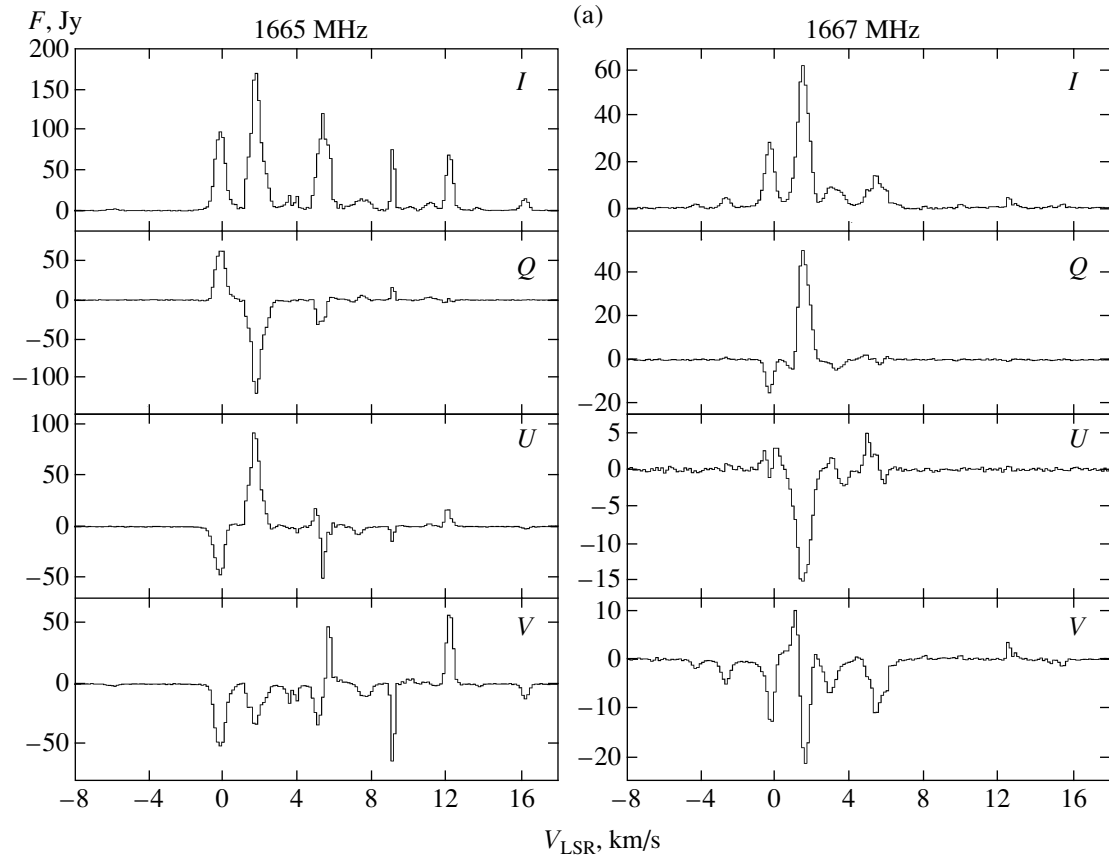


**Fig. 1.** Spectra of the Stokes parameters of the OH lines in W75N for October 27, 2007. Horizontal axis is the radial velocity relatively to the Local standard of rest; vertical axis is the flux density.

The source W75N (G81.871+0.781) is located in the massive-star-formation complex Cygnus X, located about 2 kpc from the Sun. It includes a number of dense gas–dust clouds, compact HII regions around massive young stars, and maser radio sources radiating in lines of hydroxyl (OH), water ( $H_2O$ ), and methanol ( $CH_3OH$ ). OH maser emission in W75N was first observed by Zuckerman et al. [10] in 1968. The OH emission of W75N turned out to be strongly variable; its variability on various time intervals was studied in [9, 11, 12]. Interferometric observations of the OH masers in W75N were carried out in [4–8, 13–22]. The OH masers in the W75N region are concentrated in two activity centers associated with radio continuum sources—the compact HII regions VLA 1 and VLA 2.

A model of the magnetic field in W75N based on interferometric observations of OH masers was considered in [23, 24]. Gray et al. [23] suggested the presence of a rotating molecular disk that hosts the maser condensations around the central object in VLA 1. According to the model [23], the intensity and direction of the magnetic field found from interfero-

metric maps in lines of the OH ground state  $^2\Pi_{3/2}$ ,  $J = 3/2$  ( $\lambda = 18$  cm) [21] correspond to twisted field lines in a rotating disk. Fish et al. [24] deduced two preferred directions of the magnetic field near VLA 1 from observations in lines of the excited OH state  $^2\Pi_{3/2}$ ,  $J = 5/2$  ( $\lambda = 5$  cm): North–South and East–West. The magnetic fields derived in these papers are  $\sim 8$  mG.

On the VLBA map of the OH maser W75N [19] obtained on July 1, 1998, the maser condensations form an elongated arc encompassing the radio continuum source VLA 1, consistent with the circumstellar-disk model. There are pairs of spatially coincident emission features with opposite directions of circular polarization. These pairs were used by Slysh et al. [19] to measure the corresponding magnetic fields, which were found to be 5.2 and 7.7 mG for the two pairs of features “A–B” in the 1665 MHz line and “M–O” in the 1667 MHz line, respectively.

A strong magnetic field in W75N was measured in [22]. A number of Zeeman features were detected on VLBA maps of W75N obtained for January 1, 2001 in

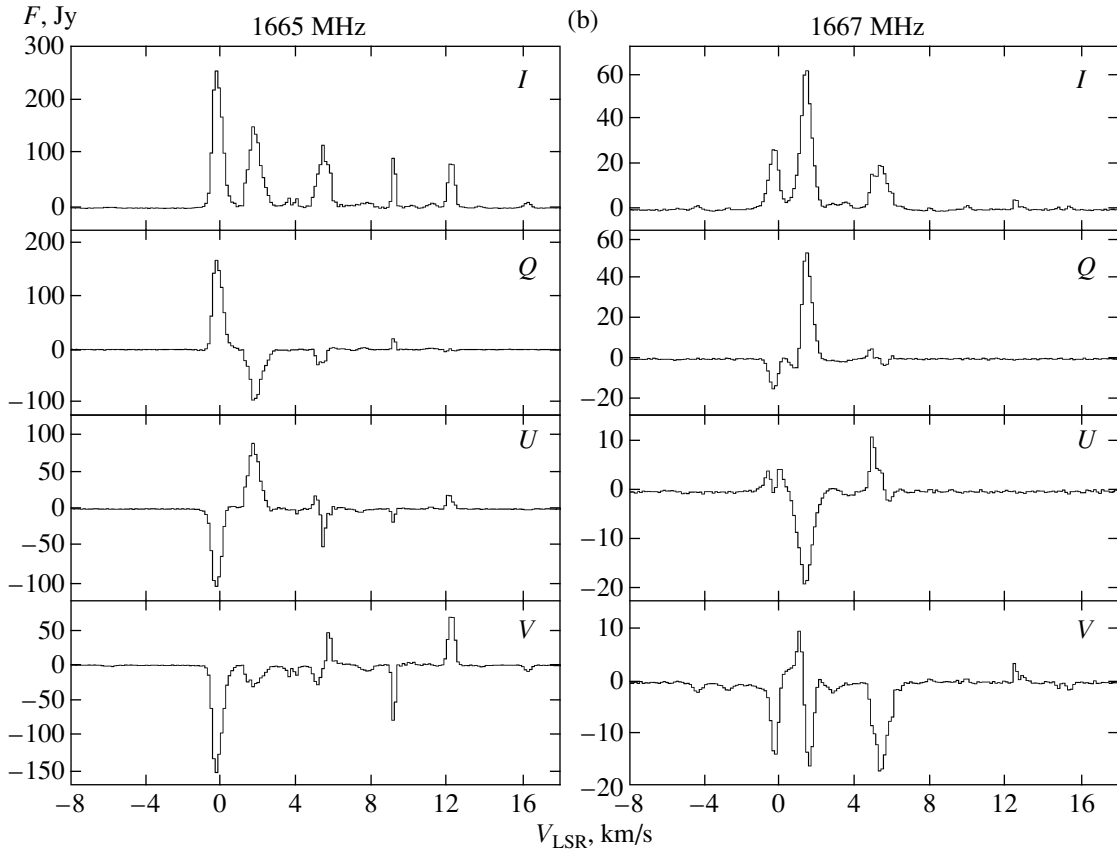


**Fig. 1.** (Contd.) Same as Fig. 1a for November 17, 2007.

the 1665 and 1667 MHz OH lines, implying magnetic fields reaching values of 40 mG [22].

Here, we report new results of monitoring the flux density and total polarization of the maser emission in the 1665 and 1667 MHz OH lines ( $\lambda = 18$  cm) in the star-forming region W75N obtained on the Nançay radio telescope (France).

## 2. ZEEMAN EFFECT IN THE MASER LINES

In a magnetic field, the main OH lines at 1665 and 1667 MHz are split into three components: the unshifted  $\pi$  component, which is linearly polarized, and two  $\sigma$  components shifted up and down in frequency, which are elliptically polarized in opposite directions [1, 2]. In a longitudinal field with intensity  $B$ , the frequency separation between the  $\sigma$  components is [2]

$$\Delta\nu = \frac{5}{2} \frac{g_J\mu_0}{h} B \quad (1)$$

for the 1665 MHz line,

$$\Delta\nu = \frac{3}{2} \frac{g_J\mu_0}{h} B \quad (2)$$

for the 1667 MHz line,

where  $g_J$  is the Landé factor (0.935 for both lines),  $\mu_0$  the Bohr magneton, and  $h$  Planck's constant. Numerically,  $\mu_0/h = 1.39967$  kHz mG $^{-1}$ ; the splitting between the  $\sigma$  components in radial velocity is 0.590 km s $^{-1}$  mG $^{-1}$  for the 1665 MHz line and 0.354 km s $^{-1}$  mG $^{-1}$  for the 1667 MHz line [2]. Measuring the velocity difference between the oppositely polarized  $\sigma$  components, we can determine the intensity and direction of the line-of-sight component of the magnetic field. The positions of the masers of a Zeeman pair measured in different polarizations coincide within the errors, or within fractions of a millisecond in the case of VLBI measurements. This condition follows from the nature of the Zeeman splitting: both  $\sigma$  components are emitted by each molecule simultaneously as a result of its precession in the magnetic field. In the case of a maser, full or partial suppression of one  $\sigma$  component by the other is possible [25]. VLBI observations of OH masers confirm the positional coincidence of the  $\sigma$  components, though their intensities are usually not equal.

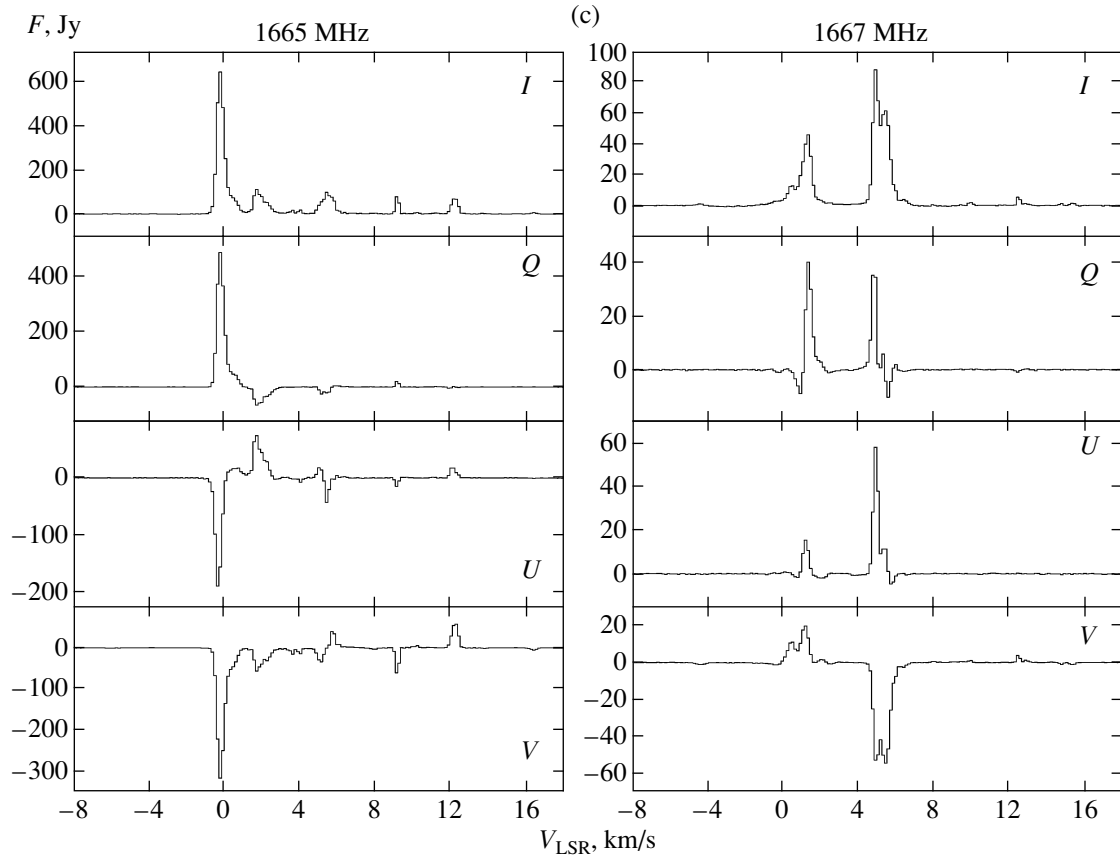


**Fig. 1.** (Contd.) Same as Fig. 1a for April 17, 2008.

### 3. OBSERVATIONS AND DATA PROCESSING

We have observed the radio source W75N in the hydroxyl lines on the radio telescope of the Nançay Radio Astronomy Observatory of the Paris–Meudon Observatory (France). This telescope is a two-mirror Kraus instrument. It is a transit telescope, providing observations near the meridian. A movable flat reflector  $200 \times 40$  m in size directs incoming radio waves onto a fixed spherical mirror  $300 \times 35$  m in size, which has a radius of curvature of 560 m and is located at a distance of 460 m. In turn, this spherical mirror focuses the radio waves onto a feed near the ground, mounted on a chariot moving along a rail track. The motion of this feed enables tracking of a radio source within  $\pm 30^\circ / \cos \delta$  in hour angle relative to the meridian. At declination  $\delta = 0^\circ$ , the telescope beam at 18 cm is  $3.5' \times 19'$  in right ascension and declination, respectively. Observations of radio sources are possible at  $\delta > -39^\circ$ . The telescope sensitivity at  $\lambda = 18$  cm and  $\delta = 0^\circ$  is 1.4 K/Jy. The noise temperature of the liquid-helium-cooled preamplifiers is from 35 to 60 K, depending on the observing conditions.

The spectral analysis is carried out by an 8192-channel autocorrelation spectrum analyzer. These channels can be divided into several batteries, each of which realizes an independent signal analysis in one of the two OH lines (1665 and 1667 MHz) and in one of four polarization modes. In our observations, the spectrum analyzer was divided into eight batteries with 1024 channels in each. The analysis frequency bandwidth of each battery was 781.25 kHz, and the frequency resolution was 763 Hz, corresponding to a radial-velocity resolution of 0.137 km/s in the 1665 and 1667 MHz lines.

A recent upgrade has extended the capabilities of polarization observations [26]. New observations conducted by us in 2007–2009 appreciably supplement earlier polarization studies performed with the Nançay radio telescope. The radio telescope simultaneously receives two orthogonal modes of linear polarization, directly yielding the intensities of the corresponding linear modes ( $L0^\circ$ ,  $L90^\circ$ ). Mixing the signals from the orthogonal feeds delaying the phase of one mode by a quarter of the wavelength also yields two orthogonal circular modes ( $LC1$ ,  $RC1$ ). Thus, the three Stokes parameters  $I$ ,  $V$ , and  $Q$  are observed

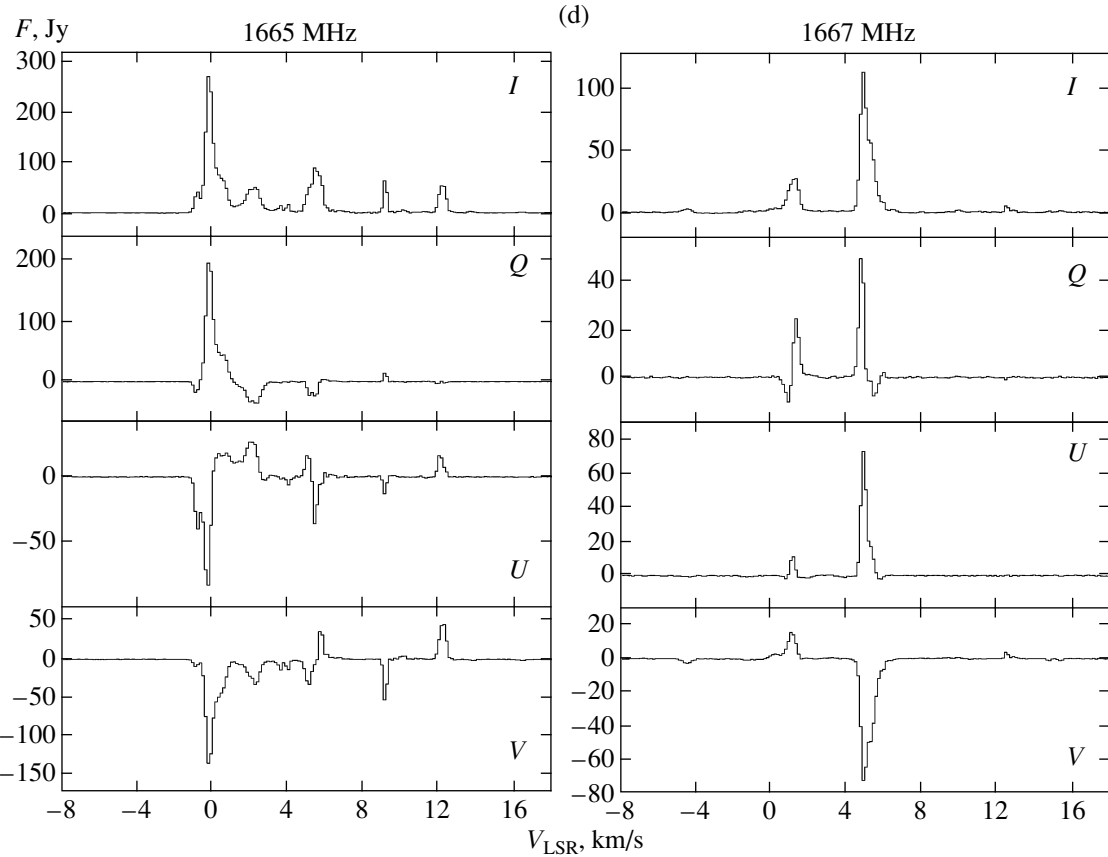


**Fig. 1.** (Contd.) Same as Fig. 1a for July 20, 2008.

simultaneously (with an appropriate choice of coordinate system). Further observations rotating the feeds by  $-45^\circ$  provide information on the intensity of linear modes with polarization planes inclined  $-45^\circ$  and  $45^\circ$  to the initial planes, together with two new circular modes RC2 and LC2. This enables the reconstruction of the full polarization state of the source, since we now observe Stokes parameter  $U$  instead of  $Q$  (in the same coordinate system), so that all four Stokes parameters are measured. As a result, eight quantities are observed for each frequency channel, whereas the polarization of the emission is completely described by only four Stokes parameters. Thus, the data obtained are redundant.

Combining the polarization modes, we can measure all four Stokes parameters of the OH maser emission. The Stokes parameters are determined from the flux densities  $F$  of the various polarizations in each frequency channel of the spectrum analyzer as follows [26]:

$$I = F(0^\circ) + F(90^\circ) = F(\text{RC}) + F(\text{LC}),$$

$$Q = F(0^\circ) - F(90^\circ),$$

$$U = F(45^\circ) - F(-45^\circ),$$

$$V = F(\text{RC}) - F(\text{LC}).$$

The degree of linear polarization is

$$m_L = \frac{\sqrt{Q^2 + U^2}}{I},$$

the position angle of the linear polarization is

$$\chi = \frac{180^\circ}{\pi} \arctan \left( \frac{U}{Q} \right),$$

and the degree of circular polarization is

$$m_C = \frac{V}{I}.$$

When obtaining polarization data from the radio telescope, special attention should be paid to the calibration of the so-called instrumental polarization. Most often, a calibration source with known polarization properties is observed alternately with the studied source. However, due to time limitations, observations of calibration sources are not always possible and/or justified. However, even if no observations of a calibration source are available, the instrumental polarization can be retrieved via self-calibration of the data, which is possible due to the redundancy of the

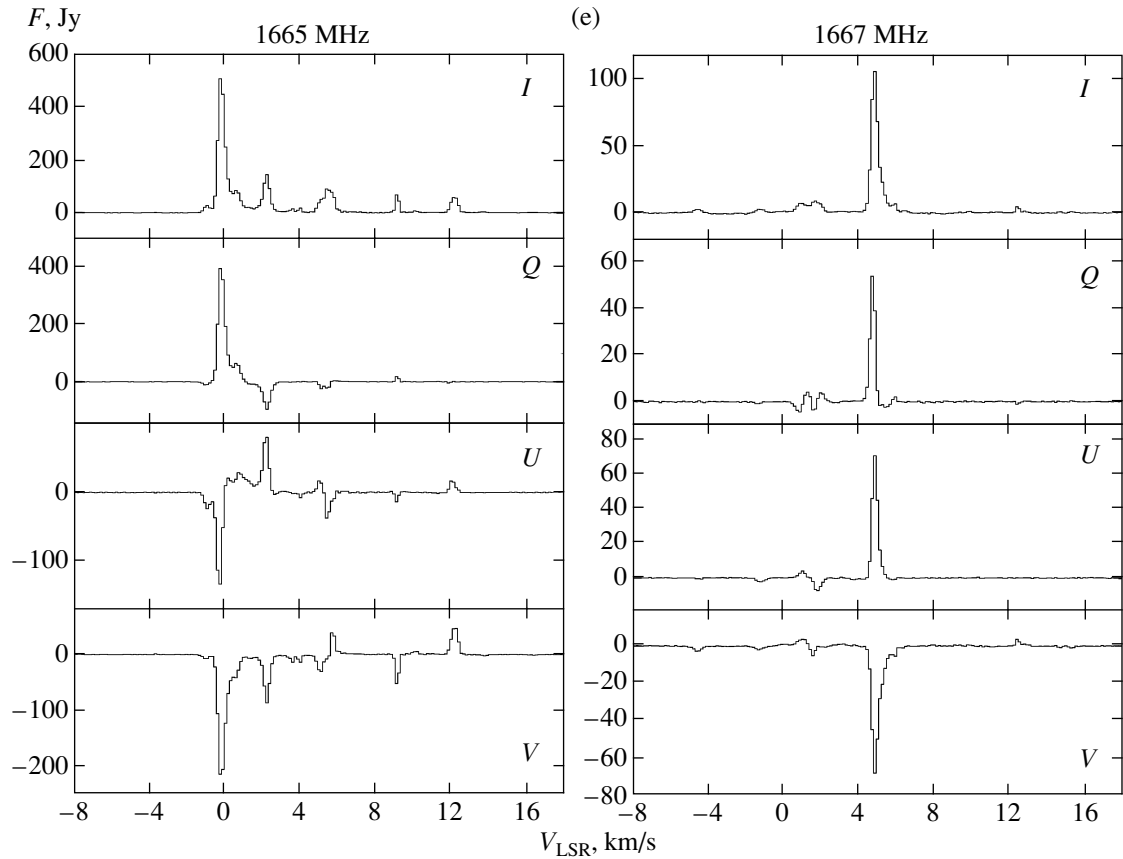


**Fig. 1.** (Contd.) Same as Fig. 1a for September 16, 2008.

data obtained from the radio telescope. If we assume that neither the observed sources nor the telescope parameters responsible for the main instrumental errors display appreciable variability on timescales of 10–20 min (the characteristic time of the observations), we can use the data redundancy to calibrate the instrumental polarization. In practice, due to the non-zero transverse dimensions of the feed and errors in the position angle, it is not possible for the feed to receive a strictly preset linear-polarization mode. When considering the “contamination” of the main received modes, we can assume in the simplest case that, in addition to the main mode, the feed receives a small fraction of the orthogonal mode. In the literature, this is known as the “ $D$ -terms model”; see, e.g., [27]. Let us write the field intensities in the mutually orthogonal feeds A and B, with the  $x$  axis of the coordinate system along the plane of the main mode of feed A and the  $z$  axis along the line of sight toward the source:

$$E_0 = L_x + D_A L_y, \quad (3)$$

$$E_{90} = -D_B L_x + L_y,$$

$$\begin{aligned} E_{-45} &= \frac{1}{\sqrt{2}}[(D_A + 1)L_x + (D_A - 1)L_y], \\ E_{+45} &= \frac{1}{\sqrt{2}}[(1 - D_B)L_x + (1 + D_B)L_y], \end{aligned}$$

where  $D$  is the fractional contamination of the main mode by the orthogonal mode. According to the definition of the Stokes parameters  $I$ ,  $Q$ , and  $U$  (see, e.g., [28, 29]),

$$I = \langle L_x L_x^* \rangle + \langle L_y L_y^* \rangle, \quad (4)$$

$$Q = \langle L_x L_x^* \rangle - \langle L_y L_y^* \rangle, \quad U = \langle L_x L_y^* \rangle - \langle L_y L_x^* \rangle,$$

the received intensities of the corresponding modes can be written in this model as

$$L_0 = G_0 \langle E_0 E_0^* \rangle = G_0 [\langle L_x L_x^* \rangle \quad (5)$$

$$+ D_A \langle L_x L_y^* \rangle + D_A \langle L_y L_x^* \rangle + D_A^2 \langle L_y L_y^* \rangle],$$

$$L_{90} = G_{90} \langle E_{90} E_{90}^* \rangle = G_{90} [D_B^2 \langle L_x L_x^* \rangle]$$

$$- D_B \langle L_x L_y^* \rangle - D_B \langle L_y L_x^* \rangle + \langle L_y L_y^* \rangle],$$

$$L_{-45} = G_{-45} \langle E_{-45} E_{-45}^* \rangle$$

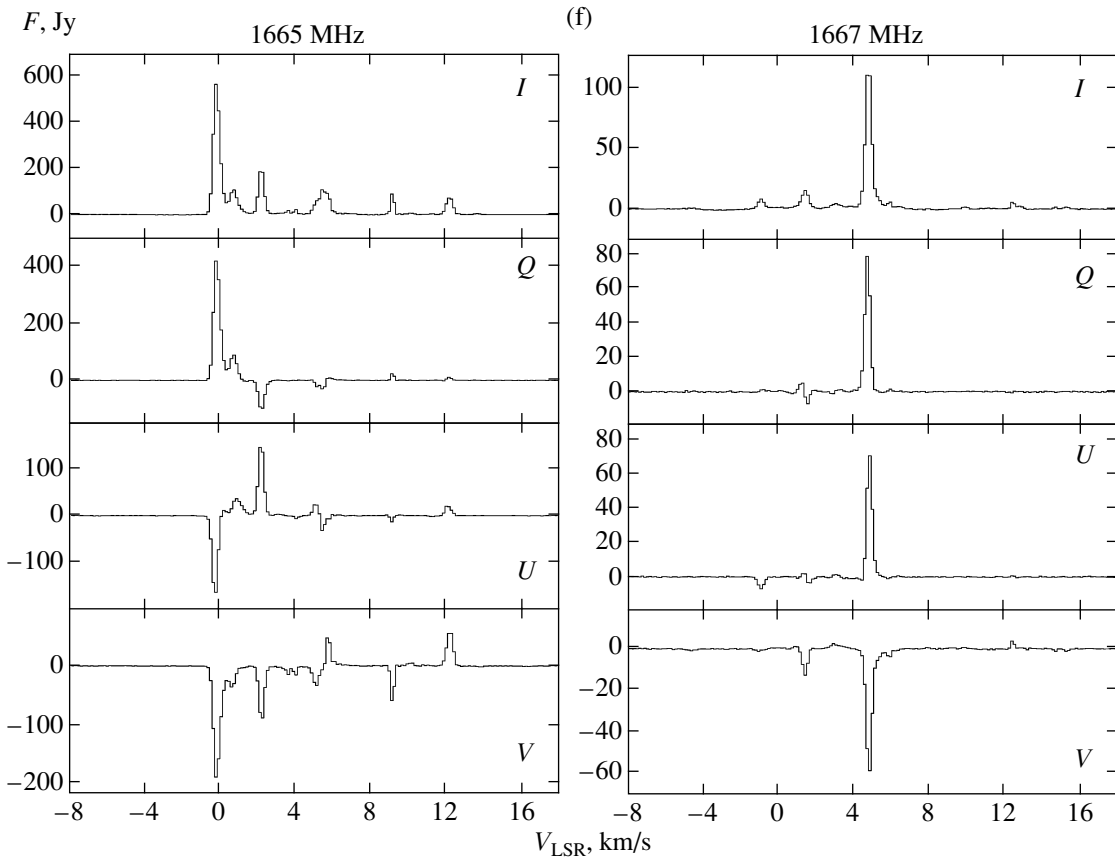


**Fig. 1.** (Contd.) Same as Fig. 1a for December 5, 2008.

$$\begin{aligned}
 &= \frac{1}{2}G_{-45}[(D_A^2 + 2D_A + 1)\langle L_x L_x^* \rangle \\
 &\quad + (D_A^2 - 1)(\langle L_x L_y^* \rangle + \langle L_y L_x^* \rangle) \\
 &\quad + (D_A^2 - 2D_A + 1)\langle L_y L_y^* \rangle], \\
 L_{+45} &= G_{+45}\langle E_{+45} E_{+45}^* \rangle \\
 &= \frac{1}{2}G_{+45}[(D_B^2 - 2D_B + 1)\langle L_x L_x^* \rangle \\
 &\quad - (D_B^2 - 1)(\langle L_x L_y^* \rangle + \langle L_y L_x^* \rangle) \\
 &\quad + (D_B^2 + 2D_B + 1)\langle L_y L_y^* \rangle],
 \end{aligned}$$

where the  $G$ 's are the instrumental gains of the receivers. In general, rotation of the feed can change the gain factor (for instance, the position of a source relative to the antenna beam obviously changes); therefore, the factors  $G_0$ ,  $-G_{-45}$ ,  $G_{90}$ , and  $G_{+45}$  are not pairwise equal, though they are obviously not independent. We intentionally do not present expressions for the measured values of the circular polarization modes, since they are derived by hybridization of the measured electric-field intensities at the orthogonal

feeds (with a shift by a quarter of the wavelength). Though the expressions for each measured component can be readily obtained in a similar way, each contains several instrumental transfer factors, as well as terms responsible for the instrumental delay of the phases of the mixed signals. This strongly complicates the problem of self-calibration. Nevertheless, we study the possibility of using the redundancy of the information received by the radio telescope to calibrate the circular polarization (the results will be published later). Neglecting second-order terms in  $D$  in the above expressions and substituting the expressions for the Stokes parameters, we find:

$$\begin{aligned}
 L_0 &= G_0 \left[ \frac{1}{2}(I + Q) + D_A U \right], \\
 L_{90} &= G_{90} \left[ \frac{1}{2}(I - Q) - D_B U \right], \\
 L_{-45} &= G_{-45} \left[ \frac{1}{2}(I - U) + D_A Q \right], \\
 L_{+45} &= G_{+45} \left[ \frac{1}{2}(I + U) + D_B Q \right].
 \end{aligned} \tag{6}$$

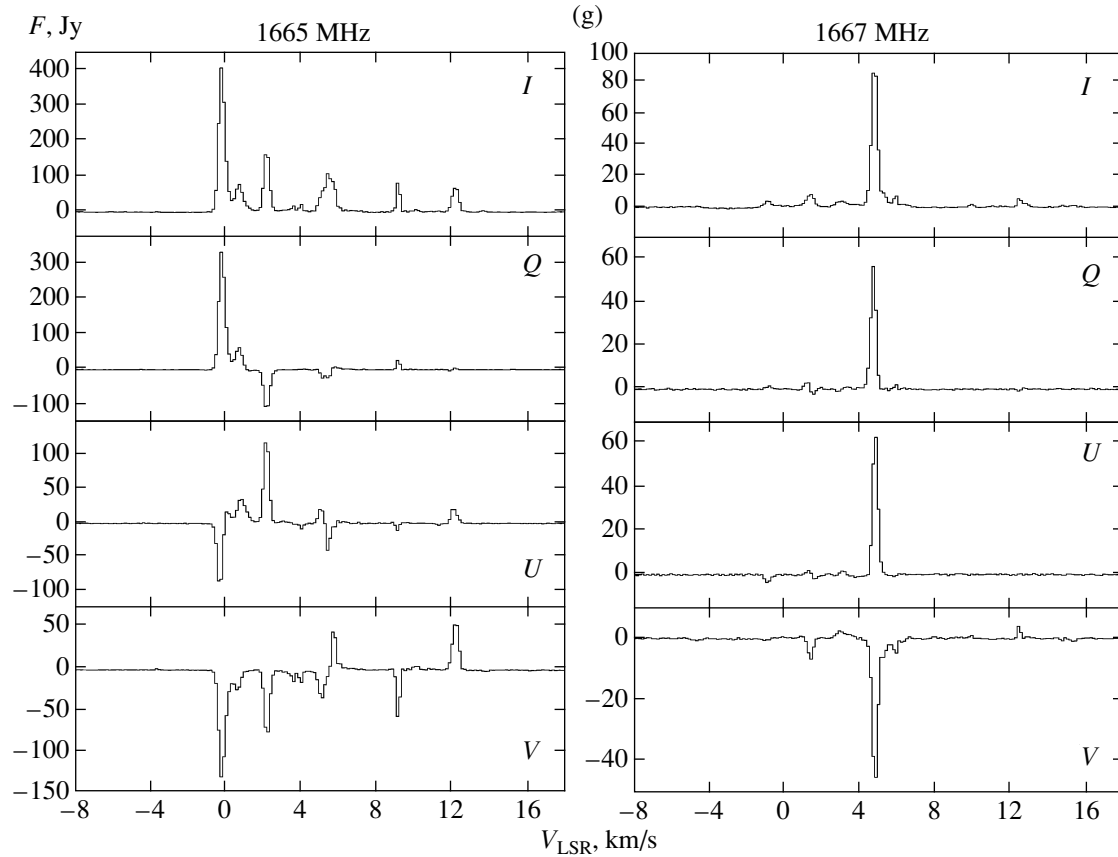


**Fig. 1.** (Contd.) Same as Fig. 1a for December 13, 2008.

Thus, even after calibrating the absolute intensities (i.e., the transfer factors  $G$ ) with an artificial unpolarized calibration source, the  $D$ -terms remain uncalibrated, and distort the observed polarization pattern. We can see from the above equations that, for a specified spectral channel, the number of unknowns is one greater than the number of observed quantities. However, if we assume that the  $D$ -terms are essentially constant throughout the observed frequency band (in the case of the Nançay radio telescope, the relative bandwidth is  $d\nu/\nu \sim 2 \text{ MHz}/1666 \text{ MHz} \sim 0.001$ ), the situation changes: the number of unknowns becomes less than the number of observed quantities. This can be used to determine the  $D$ -terms and refined Stokes parameters. However, note that the problem remains poorly constrained if the number of observed spectral features within the frequency band is small (and the problem is underdetermined if there is only one feature in the band), since it is logical to assume constancy of the polarization state within a single feature and, consequently, of the dependence of the Stokes parameters and observed polarization modes. To find the Stokes parameters in each frequency channel and the  $D$ -terms common

for the entire frequency band (or frequency intervals), we can use the least-squares method after linearizing the above equations in the required parameters  $I$ ,  $Q$ ,  $U$ ,  $D_A$ , and  $D_B$ . We initially estimate the  $D$ -terms to be zero, and use the values uncorrected for the instrumental polarization as initial estimates of the Stokes parameters:

$$I_0 = \frac{1}{2}(L_0 + L_{90} + L_{+45} + L_{-45}), \quad (7)$$

$$Q_0 = L_0 - L_{90}, \quad U_0 = L_{+45} - L_{-45}.$$

In this case, the least-squares minimization reduces to solving a system of linear algebraic equations in the corrections to  $I$ ,  $Q$ ,  $U$ ,  $D_A$ , and  $D_B$ . The obtained corrections are applied to the parameters, which then represent the initial estimates for the next least-squares iteration; the process is repeated until the required solution accuracy is achieved. For a small number of spectral features, the problem of simultaneously searching for  $I$ ,  $Q$ ,  $U$ ,  $D_A$ , and  $D_B$  is poorly constrained; therefore, in this case, it is more expedient to find only  $D_A$  and  $D_B$ , and to estimate the

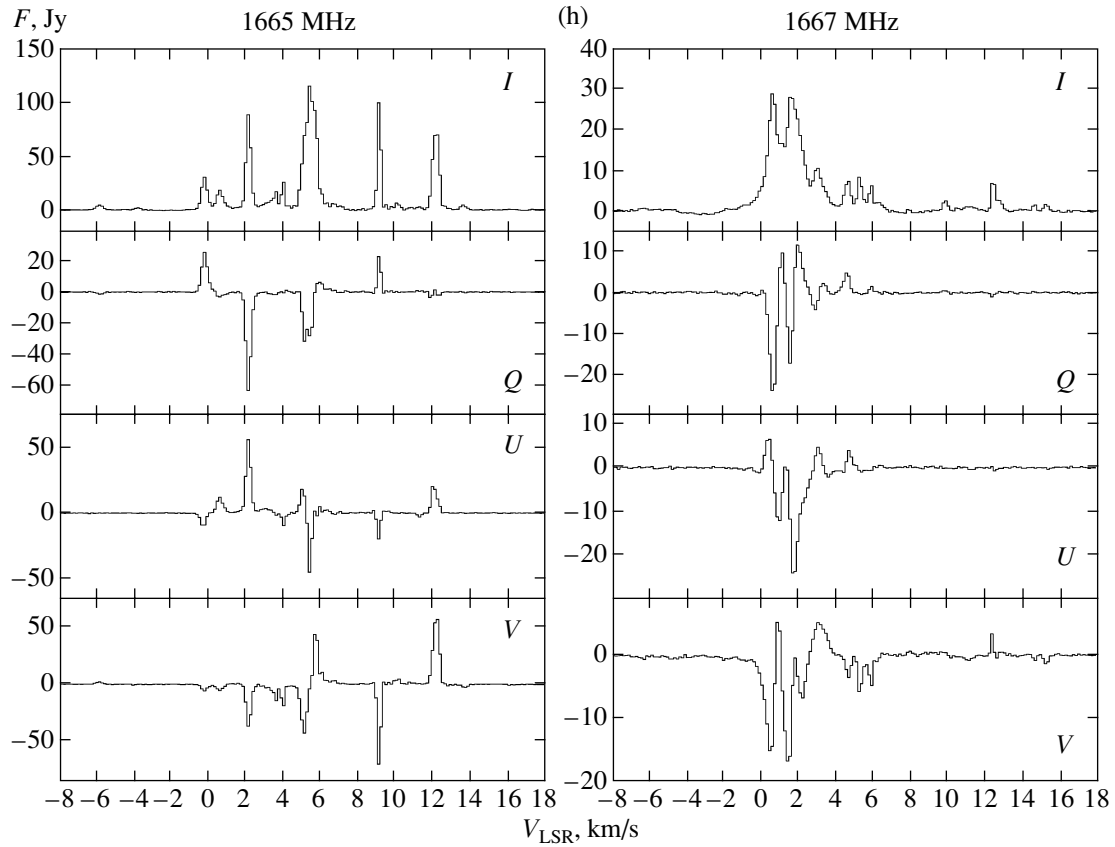


**Fig. 1.** (Contd.) Same as Fig. 1a for March 20, 2009.

Stokes parameters using the formulas

$$\begin{aligned} I_{n+1} &= \frac{1}{2}(L_0 + L_{90} + L_{+45} + L_{-45}) & (8) \\ &+ (D_{A,n} - D_{B,n})(U_n + Q_n), \\ Q_{n+1} &= L_0 - L_{90} + (D_{A,n} + D_{B,n})U_n, \\ U_{n+1} &= L_{+45} - L_{-45} - (D_{A,n} + D_{B,n})Q_n. \end{aligned}$$

This technique has been applied to Nançay spectra of the linear polarization of OH maser sources (in particular, here, to W75N). This has made it possible to reduce the influence of instrumental effects on the measured profiles of the Stokes parameters.

#### 4. RESULTS

Figure 1 shows the resulting spectra of the Stokes parameters for the 1665 and 1667 MHz lines toward W75N for 2007–2009. Figure 2 shows flux-density variations for the three spectral features that displayed the strongest variability. The high degree of both linear and circular polarization is obvious. We observed a flare of the 1665 MHz maser feature at  $V_{\text{LSR}} = -0.25$  km/s. The flux density of this feature

began to increase between October 27 and November 17, 2007. In the spectrum for April 17, 2008, the peak flux density of the feature reached 650 Jy (Fig. 1c). In the spectrum for July 20, the flux density fell to 270 Jy, increasing again to 506 Jy by September 16. By December 13, 2008, the flux density of the feature had gradually decreased, and had fallen to 30 Jy by March 20, 2009. The features at +2 km/s (1665 MHz) and +5.5 km/s (1667 MHz) varied synchronously, while flux densities of other features remained virtually unchanged. All three features again experienced a powerful flare within a short time interval (before April 13, 2009): the feature at -0.25 km/s (1665 MHz) grew to 736 Jy, the feature at +2 km/s (1665 MHz) increased from 43 to 310 Jy, and the feature at +5.5 km/s (1667 MHz) from 8 to 27 Jy. Again, the intensities of other features in the spectrum remained essentially unchanged (Figs. 1h, 1i).

A flare of the 1665 MHz line in W75N also occurred in 2003–2004 at  $V_{\text{LSR}} = 2$  km/s, when the flux density reached 800 Jy and W75N became for some time the brightest OH maser in the sky [9, 12]. This flare, together with the two flares observed by us in 2008–2009, could be related to the same

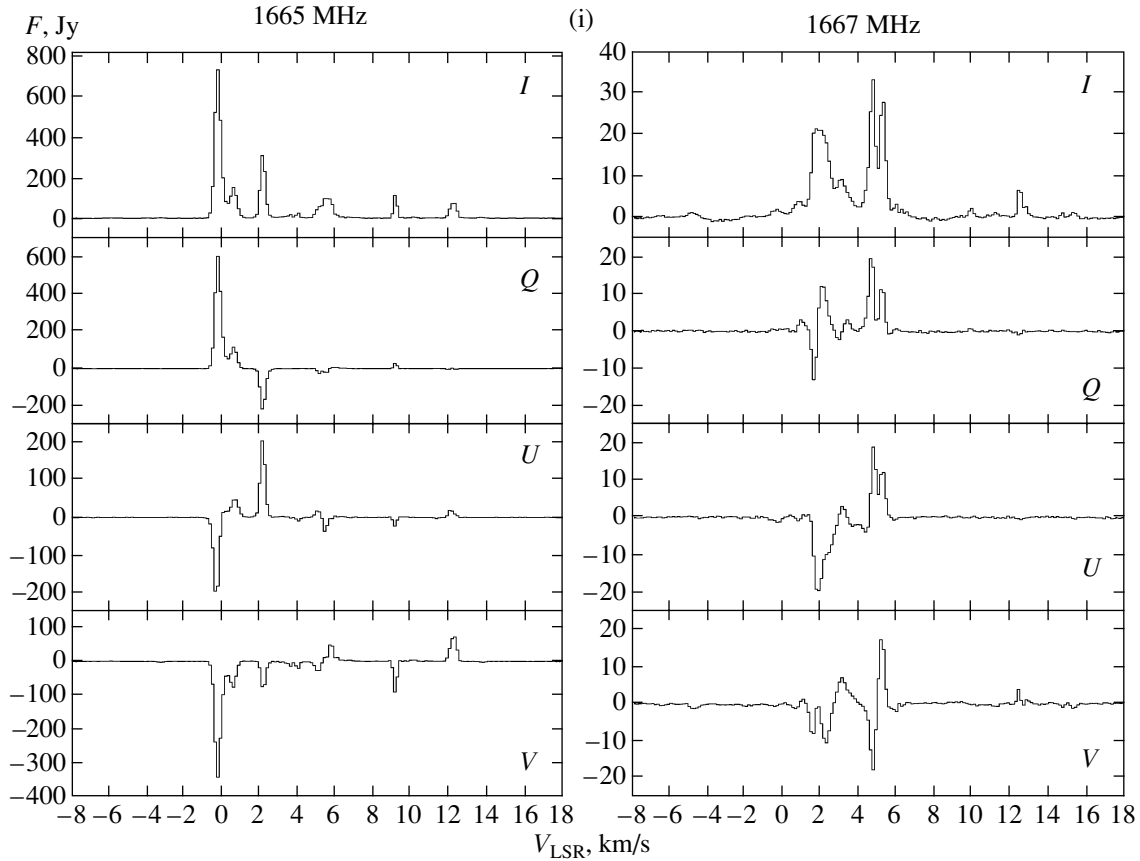


**Fig. 1.** (Contd.) Same as Fig. 1a for April 13, 2009.

phenomenon, possibly the consecutive passage of an MHD shock from the central star across several different maser condensations. Strong flares in W75N were also observed in the  $\lambda = 1.35$  cm H<sub>2</sub>O line [30, 31].

We detected Zeeman splitting in the profile of Stokes  $V$  at  $V_{\text{LSR}} = +5.5$  km/s in the 1667 MHz line, which appeared between March 20 and April 13, 2009. In our 1667 MHz profile, this feature approximately corresponds in radial velocity to the emission feature “O” near VLA 1 on the map of W75N of Slysh et al. [19]; the feature “M” at  $V_{\text{LSR}} = +8.65$  km/s, which formed a Zeeman pair with “O” [19], is absent in our profile for April 13, 2009. Feature “O” displayed strong circular polarization ( $m_C = 0.925$ ) in [19]. In our observations, we found a relative shift of two strongly circularly polarized  $\sigma$  components in the  $V$  profile, with opposite signs and with  $m_C = 0.5–0.7$ . The splitting between the  $\sigma$  components is 0.4 km/s. According to (2), this splitting corresponds to a line-of-sight component of the magnetic field of  $-1.1$  mG (the minus sign means that the component is directed away from the observer). The high frequency resolution of our observations enabled us to detect and

measure this small Zeeman splitting, which corresponds to a magnetic field appreciably weaker than that measured in W75N previously.

## 5. CONCLUSIONS

We have observed the maser emission in the 1665 and 1667 MHz OH lines from the high-mass star-formation region in W75N at nine epochs in 2007–2009 using the radio telescope of the Nançay Radio Astronomy Observatory. We have developed and applied a technique for correcting for the instrumental polarization. The circular and linear (elliptical) polarization of the OH maser emission in W75N testifies to the presence in this star-forming region of a magnetic field that is strong enough (of the order of a few milligauss) to split the maser lines into separate Zeeman components. The field may be enhanced by compression of the circumstellar gas under the action of the stellar wind from a young star (for instance, via MHD shocks). During the 1.5 years of our observations, we observed two strong flares of maser features at  $V_{\text{LSR}} = -0.25$  and  $+2$  km/s in the 1665 MHz line and at  $+5.5$  km/s in the 1667 MHz line. Inspection of

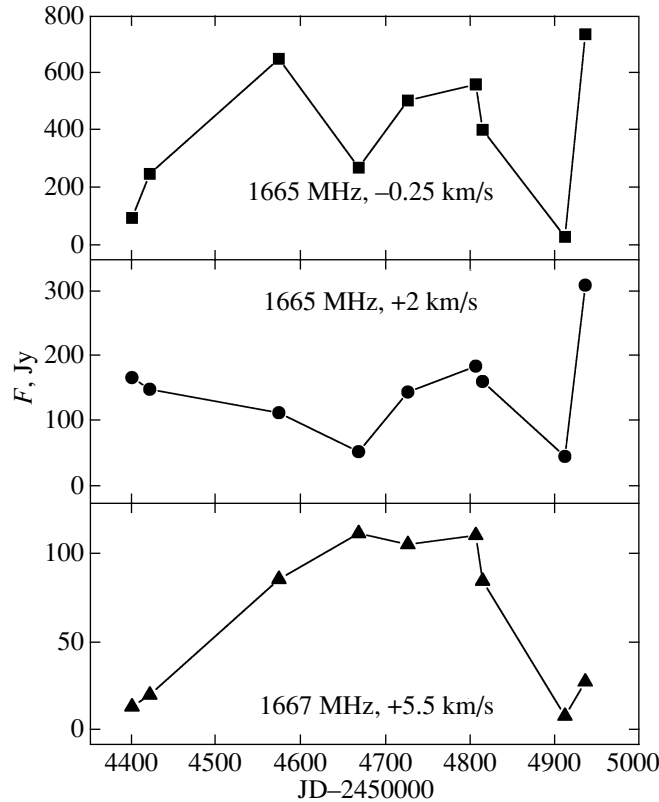


**Fig. 2.** Time dependence of the peak flux density for three OH spectral features in W75N.

the OH line profiles demonstrates that these features also have the greatest degrees of polarization. Using the splitting between the  $\sigma$  components in the Stokes  $V$  profile of the emission feature at  $V_{\text{LSR}} = +5.5 \text{ km/s}$  in the 1667 MHz line, we have estimated the intensity of the line-of-sight component of the magnetic field to be  $-1.1 \text{ mG}$ . A maser flare between March 20 and April 13, 2009 (Fig. 2) may be related to the compression of material at a shock front.

#### ACKNOWLEDGMENTS

The authors thank the staff of the Nançay Radio Astronomy Observatory for their help with the observations. One of the authors (V.M.V.) gratefully acknowledges a grant of the President of the Russian Federation for the State Support of Young Russian PhD Scientists (MK-2839.2009.2). This work was supported by the Russian Foundation for Basic Research (project no. 06-02-16806-a).

#### REFERENCES

1. D. A. Varshalovich and V. V. Burdyuzha Astron. Zh. **52**, 1178 (1975) [Sov. Astron. **19**, 705 (1976)].
2. R. D. Davies, in *Galactic Radio Astronomy*, Ed. by F. J. Kerr and S. C. Simonson (Reidel, Dordrecht, Holland, Boston, 1974), p. 275.
3. H. E. Radford, Phys. Rev. **122**, 114 (1961).
4. A. L. Argon, M. J. Reid, and K. M. Menten, Astrophys. J. Suppl. Ser. **129**, 159 (2000).
5. V. L. Fish, M. J. Reid, A. L. Argon, and K. M. Menten, Astrophys. J. **596**, 328 (2003).
6. V. L. Fish, M. J. Reid, A. L. Argon, and X.-W. Zheng, Astrophys. J. Suppl. Ser. **160**, 220 (2005).
7. V. L. Fish and M. J. Reid, Astrophys. J. Suppl. Ser. **164**, 99 (2006).
8. V. L. Fish and M. J. Reid, Astrophys. J. **656**, 952 (2007).
9. M. Szymczak and E. Gérard, Astron. Astrophys. **494**, 117 (2009).
10. B. Zuckerman, D. F. Dickinson, J. A. Ball, et al., Astron. J. **73**, S210 (1968).
11. W. T. Sullivan, III and J. H. Kerstholt, Astron. Astrophys. Suppl. Ser. **26**, 399 (1976).
12. A. V. Alakoz, V. I. Slysh, M. V. Popov, and I. E. Val'tts, Pis'ma Astron. Zh. **31**, 422 (2005) [Astron. Lett. **31**, 375 (2005)].
13. P. J. Harvey, R. S. Booth, R. D. Davies, et al., Mon. Not. R. Astron. Soc. **169**, 545 (1974).
14. N. J. Evans, II, R. M. Crutcher, and W. J. Wilson, Astrophys. J. **206**, 440 (1976).
15. A. D. Haschick, M. J. Reid, B. F. Burke, et al., Astrophys. J. **244**, 76 (1981).
16. R. P. Norris, R. S. Booth, P. J. Diamond, and N. D. Porter, Mon. Not. R. Astron. Soc. **201**, 191 (1982).

17. E. E. Baart, R. J. Cohen, R. D. Davies, et al., Mon. Not. R. Astron. Soc. **219**, 145 (1986).
18. V. I. Slysh, I. E. Val'tts, and V. Migenes, Astron. Zh. **78**, 1073 (2001) [Astron. Rep. **45**, 942 (2001)].
19. V. I. Slysh, V. Migenes, I. E. Val'tts, et al., Astrophys. J. **564**, 317 (2002).
20. V. I. Slysh, I. E. Val'tts, and V. Migenes, Astron. Zh. **79**, 240 (2002) [Astron. Rep. **46**, 216 (2002)].
21. B. Hutawarakorn, R. J. Cohen, and G. C. Brebner, Mon. Not. R. Astron. Soc. **330**, 349 (2002).
22. V. I. Slysh and V. Migenes, Mon. Not. R. Astron. Soc. **369**, 1497 (2006).
23. M. D. Gray, B. Hutawarakorn, and R. J. Cohen, Mon. Not. R. Astron. Soc. **343**, 1067 (2003).
24. V. L. Fish, M. J. Reid, K. M. Menten, and T. Pillai, Astron. Astrophys. **458**, 485 (2006).
25. I. S. Shklovsky, Astron. Zh. **46**, 3 (1969).
26. M. Szymczak and E. Gérard, Astron. Astrophys. **423**, 209 (2004).
27. D. H. Roberts, J. F. C. Wardle, and L. F. Brown, Astrophys. J. **427**, 718 (1994).
28. G. V. Rozenberg, Usp. Fiz. Nauk **56**, 77 (1955).
29. *Physical Encyclopedia*, Ed. by A. M. Prokhorov (Bol. Ross. Entsiklop., 1994), Vol. 4, p. 690 [in Russian].
30. E. E. Lekht, V. I. Slysh, and V. V. Krasnov, Astron. Zh. **84**, 1070 (2007) [Astron. Rep. **51**, 967 (2007)].
31. E. E. Lekht, V. I. Slysh, and V. V. Krasnov, Astron. Zh. **86**, 460 (2009) [Astron. Rep. **53**, 420 (2009)].

*Translated by G. Rudnitskii*